

Effect of the chemical vapor deposition condition on the electrochemically catalytic efficiency for hydrogen evolution reaction in MoS₂ nanoparticles

Quyen Le Do, Duc Anh Nguyen *



Use your smartphone to scan this QR code and download this article

ABSTRACT

Introduction: Using the metal organic chemical vapor deposition (MOCVD) method, we have synthesized the MoS₂ nanoparticles on graphite foil substrates employed as the electrochemical working electrodes with highly efficient electrocatalysis for hydrogen evolution reaction (HER). **Methods:** The morphological and structural properties of the as-grown MoS₂ materials were demonstrated by field emission scanning electron microscope (FESEM) and Raman spectroscopies, while their elemental components were investigated by X-ray photoelectron spectroscopy (XPS). **Results:** The optimum growth time was acquired to be 11 hours. Thereby such obtained electrode exhibited the maximum HER activity with onset over the potential of 220 mV versus reversible hydrogen electrode (RHE), and the Tafel slope of 66 mV per decade (mV/dec). **Conclusion:** Our results suggest a good technique for the research of high-efficient HER electrocatalyst based on atomic-thickness layered materials.

Key words: MoS₂ nanoparticles, metal-organic chemical vapor deposition, hydrogen evolution reaction

INTRODUCTION

Hydrogen gas, an excellent source of clean energy, has been demonstrated as an ideal replacement for hydrocarbon-based and fossil fuels^{1,2}. Hydrogen gas can be conveniently yielded from the electrochemical water splitting reaction²⁻⁴. Using this approach, the hydrogen evolution reaction (HER) that happens on a cathode surface can be accelerated by loading an electrocatalyst on it. However, the best electrocatalysts for HER are Pt and its relation noble metals, which has substantially limited their commercial massive production⁴⁻⁶. Thus, developing low-cost electrocatalysts that possess strong stable and HER performance to be close to Pt-based catalysts is ultimately desirable. So far, nanostructures of molybdenum disulfide (MoS₂) have been proven promising candidates for excellent catalytic activity⁷⁻⁹. Using DFT calculation, J. K. Nørskov's group first reported that hydrogen adsorption Gibbs free energy of edge sites of MoS₂ is close to zero ($\Delta G_H \sim 0$ eV), suggesting MoS₂ probably as a great HER catalyst¹⁰. The experimental measurements then assured this prediction of HER performance of MoS₂ nanoparticles on graphite¹⁰, and Au(111) substrates¹¹. Subsequently, numerous reports have focused on maximizing the exposed active-edge-sites, aiming to enhance the HER activ-

ity of MoS₂. These efforts can be the growth of vertical nanoflakes¹², nanobelts¹³, mesoporous^{14,15}, or nanoparticles¹⁶. On the other hand, due to low intrinsic conductivity in MoS₂, one can reduce the number of layers to minimum the charge transfer resistance between the exposure surface at the outmost layer and the electrode¹⁷. In this regard, a small number of layers was demonstrated as another important expect for highly catalytic HER performance in MoS₂ nanostructure. Generally, MoS₂ nanostructure with a small number of layers (around 2~4 layers) might be a great alternative of noble-metal-based HER electrocatalysts. However, synthesis a large scale of few-layer MoS₂ nanostructure directly on conductive substantial has been still difficult¹⁸.

Here, we used the MOCVD technique to grow MoS₂ nanoparticles directly on conductive graphite, which was applied for HER electrochemical working electrode. This work focused on the dependence of HER performance on the MOCVD growing condition, particularly the growth time. We found the sample grown in 11h to exhibit the highest HER activity with the smallest onset overpotential of 250 mV/dec, and the Tafel slope of 66 mV/dec.

MATERIALS - METHODS

Department of Physics, Faculty of Basic-Fundamental Sciences, Viet Nam Maritime University, 484 Lach Tray Road, Le Chan, Hai Phong, Viet Nam.

Correspondence

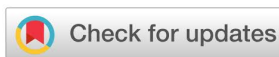
Duc Anh Nguyen, Department of Physics, Faculty of Basic-Fundamental Sciences, Viet Nam Maritime University, 484 Lach Tray Road, Le Chan, Hai Phong, Viet Nam.

Email: ducna@vimaru.edu.vn

History

- Received: 2021-02-21
- Accepted: 2021-05-05
- Published: 2021-05-13

DOI : 10.32508/stdj.v24i2.2520

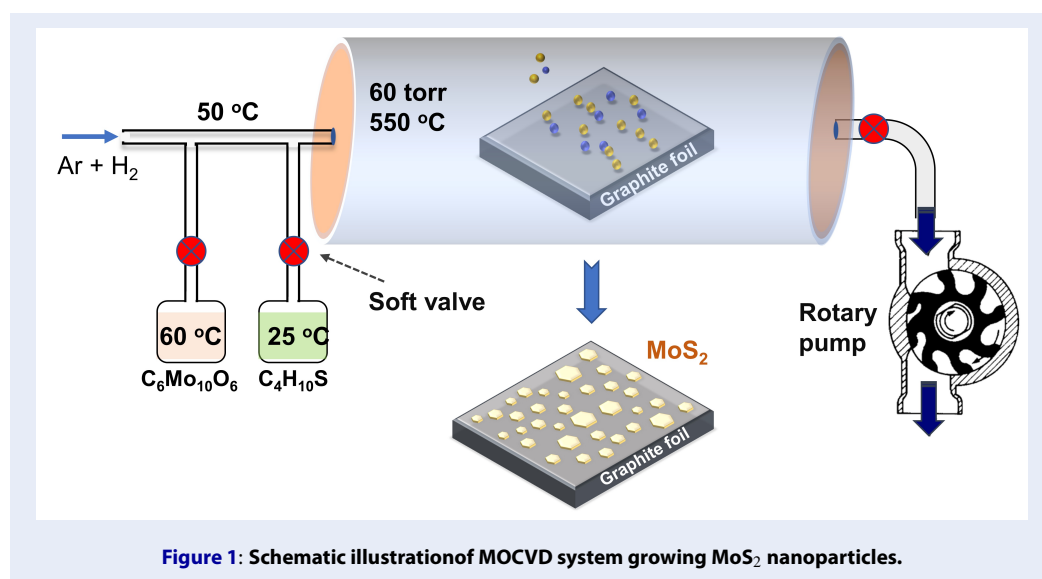


Copyright

© VNU-HCM Press. This is an open-access article distributed under the terms of the Creative Commons Attribution 4.0 International license.



Cite this article : Do Q L, Nguyen D A. **Effect of the chemical vapor deposition condition on the electrochemically catalytic efficiency for hydrogen evolution reaction in MoS₂ nanoparticles.** *Sci. Tech. Dev. J.*; 24(2):1947-1953.



Synthesis of MoS₂ nanoparticles

MoS₂ nanoparticles were synthesized via MOCVD, as schematically illustrated in **Figure 1**. Briefly, the experiment was taken place in a sealed 1-inch diameter quartz tube, and then graphite foil electrodes were placed at the center of the heated zone. The metal-organic compound of molybdenum hexacarbonyl (MHC, C₆MoO₆) and diethyl sulfide (DES, C₄H₁₀S) have high equilibrium vapor pressure were used as the gaseous precursors. Firstly, the base vacuum (~1 mtorr) was established in the chamber by a rotary pump. At the same time, the temperature of MHC and DES beaker was adapted at 25 °C and 60 °C, respectively. Then, a flow of 1 standard cubic centimeter per minute (sccm) of Ar gas was injected into DES beaker to dilution and thus facilitated the DES vapor flow. The temperature of the carrier line was fixed at 50 °C, and that of the reaction zone was 550 °C. A mixture of 30 sccm of Ar and 5 sccm of H₂ was continuously flowed into the reaction chamber during all growing processes to maintain the working pressure to be 60 torrs. Subsequently, the reaction process was started by introducing 1 sccm mix of (Ar + DES) and open soft valve of the MHC holder. For a comparative investigation of HER reactivity, MoS₂ samples were synthesized with various deposition times of 7, 9, 11, 13 h by a similar deposition condition.

Characterization

The morphology of MoS₂ samples was characterized by field-emission scanning electron microscopy (JSM-6500F, JEOL). The lattice vibrational properties

were investigated by micro-Raman spectroscopy using a 473 nm excitation source under ambient conditions. The X-ray photoelectron spectroscopy (XPS) measurements were carried out using a Theta Probe AR-XPS System (Thermo Fisher Scientific).

HER measurements

The three electrodes configuration, including graphite rod (i.e., counter electrode), Ag/AgCl (i.e., reference electrode), and MoS₂ nanoparticles on graphite foil (i.e., working electrode) was employed to plot the linear sweep voltammetry (LSV) and cyclic voltammetry (CV). All the electrochemical measurement was put in a 0.5 M H₂SO₄ electrolyte and was established in an electrochemical workstation (IviumStat, Ivium Tech) to study the HER reactivity.

RESULTS

The morphology of MoS₂ nanoparticles was observed by FESEM images, as shown in **Figure 2**. As shown in **Figure 2a** and **b**, the 6h grown sample is similar to the blank substrate, indicating that before 6h, the MoS₂ has not been formed in the substrate. When the growth time reaches 7h (**Figure 2c**), tiny particles appear with the size of 50-100 nm. According to **Figure 2d-f**, the density of the nanoparticles increased with the growth time, while the size of particles seems to be not changed.

Figure 3 shows the Raman spectra of the obtained MoS₂ samples. As shown in **Figure 3a**, two peaks located at 378.2 and 401.5 are attributed to the two typical active Raman scattering mode of E_{2g}¹ and A_{1g} vibrational modes in 2H phase of MoS₂, in which the

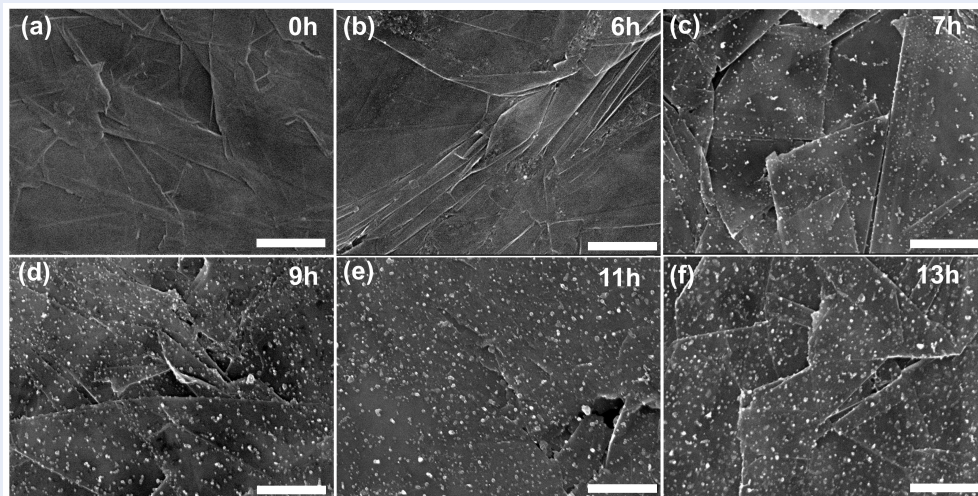


Figure 2: Morphological analysis. FESEM images of baregraphite foil (a), and MoS₂ nanoparticles (b-f) synthesized for 6, 7, 9, 11, 13 h. The scale bar is 1 μm .

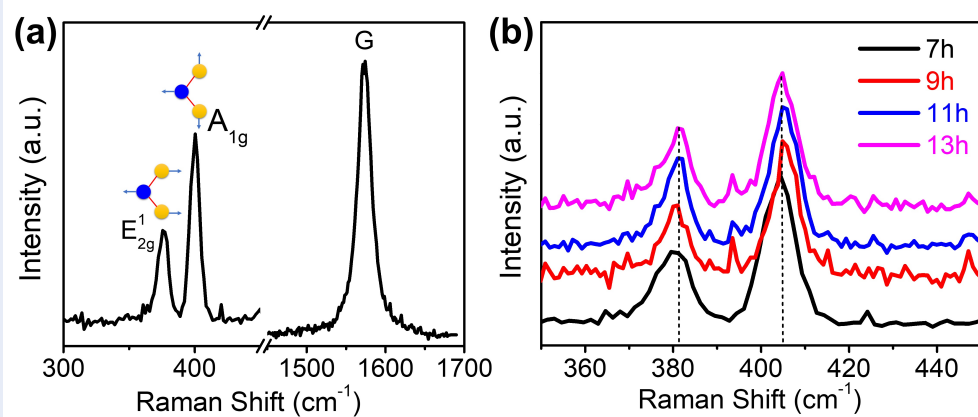


Figure 3: Raman spectra of MoS₂ nanoparticles on graphite substrate (a). The zoom-in of the Raman spectra of samples grown in 7h to 13h.

first one (E_{2g}^1) is attributed to the in-plane vibration of Mo-S bond, while the other one (A_{1g}) is corresponding to the out-of-plane vibration of S atoms¹⁹. Moreover, the frequency separation between these two peaks of 23.5 cm^{-1} suggested that the number of layers was between 3 and 4 layers^{17,20}. Although the growth time is much different (alternating between 7h~11h), the number of layers of samples does not change, reflected by the non-shift in the Raman peaks position (Figure 3b).

The X-ray photoelectron spectroscopy (see Figure 4a-b) was constructed to study the elemental bonding states of as-grown MoS₂ nanoparticles. Figure 4a illustrated the high-resolution of XPS spectra in Mo

3d region. As can be seen, the two olive-fitted peaks located at 229.65 and 232.8 eV are corresponding to Mo⁴⁺ 3d_{5/2} and Mo⁴⁺ 3d_{3/2} energy levels in MoS₂, respectively²¹. Besides, the two small peaks (orange fitted curves) overlapped at 231.8, and 235.9 eV are ascribed to the Mo⁶⁺ states, indicating the formation of a small amount of molybdenum oxide due to partial oxidation of MHC throughout the deposition process^{22,23}. Additionally, two blue fitted peaks that were detected at 162.5 and 163.7 eV (see Figure 4b) are attributed to the S²⁻ 2p_{3/2} and S²⁻ 2p_{1/2} energy states in MoS₂, respectively²³. Thus, all these data confirmed the chemical elemental composition of the fabricated materials.

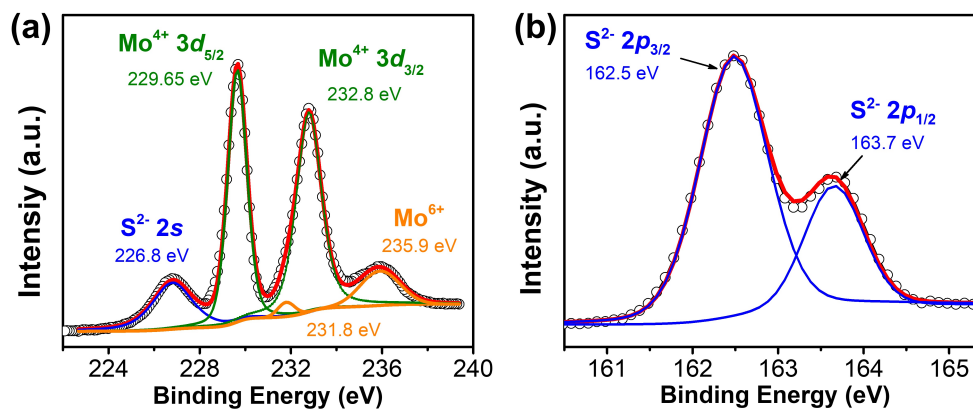


Figure 4: Chemical composition analysis. The high-resolution XPS spectroscopy of as-grown MoS₂ nanoparticles superimposed by fits (red lines) for (a) Mo 3d energy levels range: Mo⁴⁺ (olive trace), and Mo⁶⁺ (orange trace); (b) S 2p energy levels range: S²⁻ of MoS₂ (blue trace).

The HER performance was firstly examined by the linear sweep voltammetry (i.e., polarization curves), as illustrated in **Figure 5a**. As can be seen, there was a considerable enhance of HER activity as the CVD growth time increase from 7h to 11h. The 11h sample revealed the highest performance with the onset overpotential of approximately 250 mV vs. RHE, which was considerably smaller than the 7h, 13h, and bare samples. The Tafel plots can also be used to evaluate the electrocatalytic activity for HER, in which the smaller obtained Tafel slope corresponds to the higher HER reactivity. **Figure 5b** exhibited the corresponding Tafel plots of the MoS₂ nanoparticles synthesized at different times. Even though the 9h sample exhibited a similar onset overpotential with the 11h sample, its Tafel slope of 91 mV/dec was much higher than that of the 11h sample (66 mV/dec). However, when we further expanded the deposition time until 13h, the performance experienced a degeneration with the onset overpotential and the corresponding Tafel slope enlarged to ~350 mV vs. RHE and 88 mV/dec, respectively. Generally, the MoS₂ nanoparticles deposited in 11h exhibited the optimum electrochemically catalytic activity for HER.

To evaluate the density of the active site of catalysts, the cyclic voltammetry (CV) plots in a non-Faradic potential range were conducted at the scan rates changing between 10 and 70 mV/s, as shown in **Figure 5c**. Then, the double-layer capacitance (C_{dl}) obtained from the linear fitting the dependance of the average current density versus scan rates (**Figure 5d**) was demonstrated to be proportional to the active site density²⁴. As can be seen, the 11h sample exhibited

the maximum C_{dl} of 2.21 mF/cm², which is considerably larger than that of the rest ones. Thus, although the morphology and the density of MoS₂ nanoparticles of 11h and 13h samples are almost similar, the former reveals a significantly higher performance than the latter. Nevertheless, these calculations of the electrochemically active surface area of catalysts were well consistent with the above polarization curves.

Finally, the stability test for the HER catalytic activity of 11h sample was investigated by the transient chronopotentiometry measurement with a working current density of -5 mA/cm², as depicted in **Figure 5e**. During a period of 20h, we observed no significant variation of overpotential, demonstrating great stability. In addition, the nominal modification of polarization curves before and after the durability characterization verified the superior working stability of as-obtained MoS₂ nanoparticles (**Figure 5f**).

DISCUSSION

As mentioned, the MoS₂ nanoparticles that recently have been considered as a promising candidate for highly efficient electrocatalytic for HER were fabricated. Remarkably, our MOCVD method supported a direct growth of MoS₂ nanoparticles on conductive graphite foil electrodes which simplified the material preparation. The electrode surficial phenomena were tested without any extra transfer process. In this way, it also naturally avoided the electrical loss contacts for the electrochemical measurements. For catalytic HER activity, the electrochemically active sites play an essential role. Frequently, the active sites locate at the edge-sites rather than at the basal plane. As a result,

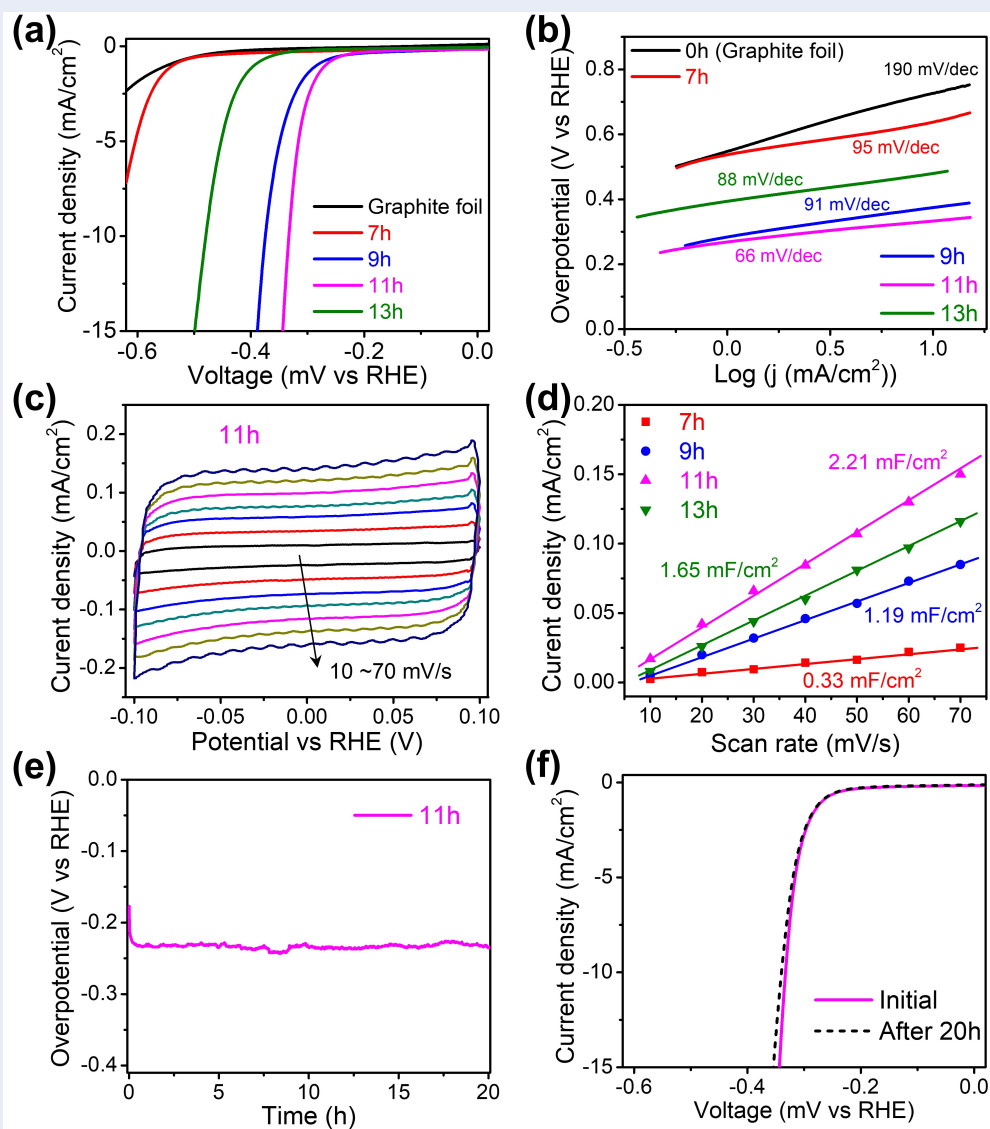


Figure 5: Electrocatalytic HER activities of MoS₂ nanoparticles. (a, b) iR-corrected LSVs and Tafel plots, respectively. (c, d) Cyclic voltammetry of the 11h sample at various scan rate, and the linearfitting of the average capacitive current density versus the scan rate for MoS₂ sample with different growth time, respectively. Stability of the obtained MoS₂ sample, (e) Potential vs. time plot, conducted at -5 mA/cm² for 11h sample, (f) LSVs of the initial 11h sample (magenta) and after applying bias states (dashed black).

ragged particles in nanoscale size are more favorable than a uniform continuous film. In addition to the morphological aspects, the thickness of MoS₂ material is another essential factor affecting total performance. The layer number ranging from 3 to 4 was demonstrated as the best option for HER reactivity¹⁶. Interestingly, the fabricated MoS₂ particles in this work well matched with above requirements.

In this study, under the same reaction temperature, carrier gas concentration, and precursors' flow rate, the morphology (i.e. size and layer number) of MoS₂

nanoparticles was similar; therefore, the catalytic activities essentially only depended on the density of particles. Meanwhile, the growth time led to the change of particle density. Thus, for the samples grown from 7 to 11h, a considerable enhancement in the electrocatalytic activity can be easily understood as extending the density of MoS₂ nanoparticles. However, we assert that a further extending growth time (≥ 13 h) should not be employed to acquire the optimum performance. We attributed the best HER performance of 11h samples to the maximum of active

site density compared to the other ones, which was then proved by the fact that it has the highest value of electrochemical double-layer capacitance (C_{dl}). One possible reason for lower performance in the more extended growth sample was a transition from the electrochemical active-Mo-edge sites to the inert S-edge sites through extra growth time²⁵. Such extra growth time might fulfill some S-vacancies existing near the active-Mo-edge sites. This mechanism should be further confirmed in the following research topic.

Finally, although the obtained performance of the present MoS₂ sample was relatively better than that of some previous MoS₂ based materials^{18,26}, it has been still far from that of Pt-based catalysts (Tafel slope ~30 mV/dec)²⁷. Therefore, some additional works are required to improve current results further. We suggest that the efficiency of MoS₂ nanoparticles can be further enhanced by activating the basal plane of MoS₂ nanoparticles by further applying surficial treatment routes, such as doping, engineering S-vacancies defect positions or hybridization with a high-surface-area substrate.

CONCLUSION

We have reported the method, namely MOCVD, to synthesize MoS₂ nanoparticles applying for the HER electrocatalysis. We found that the deposition time considerably affected the HER efficiency in which the electrochemically active sites density played an essential factor. Particularly, the 11h deposited MoS₂ sample showed the highest active site density, thereby the best HER performance with onset overpotential of 250 mV vs. RHE, and the Tafel slope of 66 mV/dec. Thus, this search may provide a straightforward and convenient route to acquire a good replacement to the Pt-based electrocatalysts.

ABBREVIATIONS

MOCVD: Metal-organic Chemical Vapor Deposition

HER: Hydrogen Evolution Reaction

RHE: Reversible Hydrogen Electrode

MHC: Molybdenum Hexacarbonyl, Mo(CO)₆

DES: Diethyl Sulfide, (C₂H₅)₂S

FESEM: Field Emission Scanning Electron Microscope

XPS: X-ray Photoelectron Spectroscopy

LSV: Linear Sweep Voltammetry

CV: Cyclic Voltammetry

COMPETING INTERESTS

The authors declare no competing interests

AUTHORS CONTRIBUTIONS

Q. L. D designed and performed the experiments. D. A. N analyzed data and wrote the manuscript. All authors have given approval to the final version of the manuscript.

ACKNOWLEDGMENTS

This work is funded by Vietnam Maritime University under grant number: "DT20-21.94".

REFERENCES

1. Cortright RD, Davda RR, Dumesic JA. Hydrogen from Catalytic Reforming of Biomass-derived Hydrocarbons in Liquid Water. *Nature*. 2002;418:964–966. PMID: 12198544. Available from: <https://doi.org/10.1038/nature01009>.
2. Turner JA. Sustainable Hydrogen Production. *Science*. 2004;305:972–974. PMID: 15310892. Available from: <https://doi.org/10.1126/science.1103197>.
3. Schlapbach L, Züttel A. Hydrogen-storage Materials for Mobile Applications. *Nature*. 2001;414:353–358. PMID: 11713542. Available from: <https://doi.org/10.1038/35104634>.
4. Zhu J, Hu L, Zhao P, Lee LYS, Wong KY. Recent Advances in Electrocatalytic Hydrogen Evolution Using Nanoparticles. *Chem. Rev*. 2020;120:851–918. PMID: 31657904. Available from: <https://doi.org/10.1021/acs.chemrev.9b00248>.
5. Voiry D, Shin HS, Loh KP, Chhowalla M. Low-dimensional catalysts for hydrogen evolution and CO₂ reduction. *Nat. Rev. Chem*. 2018;2:0105. Available from: <https://doi.org/10.1038/s41570-017-0105>.
6. Zou X, Zhang Y. Noble metal-free hydrogen evolution catalysts for water splitting. *Chem. Soc. Rev.*, 2015, 44, 5148-80;PMID: 25886650. Available from: <https://doi.org/10.1039/C4CS00448E>.
7. Yang L, Liu P, Li J, Xiang B. Two-Dimensional Material Molybdenum Disulfides as Electrocatalysts for Hydrogen Evolution. *Catalysts*. 2017;7:1–18. Available from: <https://doi.org/10.3390/catal7100285>.
8. Ding Q, Song B, Xu P, Jin S. Efficient Electrocatalytic and Photoelectrochemical Hydrogen Generation Using MoS₂ and Related Compounds. *Chem*. 2016;1:699–726. Available from: <https://doi.org/10.1016/j.chempr.2016.10.007>.
9. Lu Q, Yu Y, Ma Q, Chen B, Zhang H. 2D Transition-Metal-Dichalcogenide-Nanosheet-Based Composites for Photocatalytic and Electrocatalytic Hydrogen Evolution Reactions. *Adv. Mater*. 2016;28:1917–1933. PMID: 26676800. Available from: <https://doi.org/10.1002/adma.201503270>.
10. Hinnemann B, Moses PG, Bonde J, Jørgensen KP, Nielsen JH, Horch S, Chorkendorff I, Nørskov JK. Biomimetic Hydrogen Evolution: MoS₂ Nanoparticles as Catalyst for Hydrogen Evolution. *J. Am. Chem. Soc*. 2005;127:5308–5309. PMID: 15826154. Available from: <https://doi.org/10.1021/ja0504690>.
11. Jaramillo TF, Jørgensen KP, Bonde J, Nielsen JH, Horch S, Chorkendorff I. Identification of Active Edge Sites for Electrochemical H₂ Evolution from MoS₂ Nanocatalysts. *Science*. 2007;137:100–102. PMID: 17615351. Available from: <https://doi.org/10.1126/science.1141483>.
12. Kong D, Wang H, Cha JJ, Pasta M, Koski KJ, Yao J, Cui Y. Synthesis of MoS₂ and MoSe₂ Films with Vertically Aligned Layers. *Nano Lett*. 2013;13:1341–1347. PMID: 23387444. Available from: <https://doi.org/10.1021/nl400258t>.
13. Yang L, Hong H, Fu Q, Huang Y, Zhang J, Cui X, Fan Z, Liu K, Xiang B. Single-Crystal Atomic-Layered Molybdenum Disulfide Nanobelts with High Surface Activity. *ACS Nano*, 2015, 9, 6478-6483;PMID: 26030397. Available from: <https://doi.org/10.1021/acsnano.5b02188>.
14. Kibsgaard J, Chen Z, Reinecke BN, Jaramillo TF. Engineering the Surface Structure of MoS₂ to Preferentially Expose Active Edge Sites for Electrocatalysis. *Nat. Mater*. 2012;11:963–969. PMID: 23042413. Available from: <https://doi.org/10.1038/nmat3439>.

15. Deng J, Li H, Wang S, Ding D, Chen M, Liu C, Tian Z, Novoselov KS, Ma C, Deng D, Bao X. Multiscale Structural and Electronic Control of Molybdenum Disulfide Foam for Highly Efficient Hydrogen Production. *Nat. Commun.* 2017;8:14430. PMID: 28401882. Available from: <https://doi.org/10.1038/ncomms14430>.
16. Bora S, Jung GY, Sa YJ, Jeong HY, Cheon JY, Lee JH, Kim HY, Kim JC, Shin HS, Kwak SK, Joo SH. Monolayer-Precision Synthesis of Molybdenum Sulfide Nanoparticles and Their Nanoscale Size Effects in the Hydrogen Evolution Reaction. *ACS Nano.* 2015;9:3728–3739. PMID: 25794552. Available from: <https://doi.org/10.1021/acs.nano.5b00786>.
17. Yu Y, Huang S-Y, Li Y, Steinmann SN, Yang W, Cao L. Layer-dependent Electrocatalysis of MoS₂ for Hydrogen Evolution. *Nano Lett.* 2014;14:553–558. PMID: 24397410. Available from: <https://doi.org/10.1021/nl403620g>.
18. Cwik S, Mitoraj D, Mendoza Reyes O, Rogalla D, Peeters D, Kim J, Schütz HM, Bock C, Beranek R, Devi A. Direct Growth of MoS₂ and WS₂ Layers by Metal Organic Chemical Vapor Deposition. *Adv. Mater. Interfaces.* 2018;5(1800140):1–11. Available from: <https://doi.org/10.1002/admi.201800140>.
19. Verble JL, Wieting TJ. Lattice Mode Degeneracy in MoS₂ and Other Layer Compounds. *Phys. Rev. Lett.* 1970;25:362–365. Available from: <https://doi.org/10.1103/PhysRevLett.25.362>.
20. Zeng H, Zhu B, Liu K, Fan J, Cui X, Zhang QM. Low-frequency Raman Modes and Electronic Excitations in Atomically Thin MoS₂ Films. *Phys. Rev. B.* 2012;86:241301. Available from: <https://doi.org/10.1103/PhysRevB.86.241301>.
21. Wang X, Feng H, Wu Y, Jiao L. Controlled Synthesis of Highly Crystalline MoS₂ Flakes by Chemical Vapor Deposition. *J. Am. Chem. Soc.* 2013;135:5304–5307. PMID: 23489053. Available from: <https://doi.org/10.1021/ja4013485>.
22. Lin YC, Zhang W, Huang JK, Liu KK, Lee YH, Liang CT, Chu CW, Li LJ. Wafer-scale MoS₂ Thin Tapers Prepared by MoO₃ Sulfurization. *Nanoscale.* 2012;4:6637–6641. PMID: 22983609. Available from: <https://doi.org/10.1039/c2nr31833d>.
23. Ahn C, Lee J, Kim HU, Bark H, Jeon M, Ryu GH, Lee Z, Yeom GY, Kim K, Jung J, Kim Y, Lee C, Kim T. Low-Temperature Synthesis of Large-Scale Molybdenum Disulfide Thin Films Directly on a Plastic Substrate Using Plasma-Enhanced Chemical Vapor Deposition. *Adv. Mater.* 2015;27:5223–5229. PMID: 26257314. Available from: <https://doi.org/10.1002/adma.201501678>.
24. McCrory CC, Jung S, Ferrer IM, Chatman SM, Peters JC, Jaramillo TF. Benchmarking Hydrogen Evolving Reaction and Oxygen Evolving Reaction Electrocatalysts for Solar Water Splitting Devices. *J. Am. Chem. Soc.* 2015;137:4347–4357. PMID: 25668483. Available from: <https://doi.org/10.1021/ja510442p>.
25. Wang H, Tsai C, Kong D, Chan K, Abild-Pedersen F, Nørskov JK, Cui Y. Transition-metal Doped Edge Sites in Vertically Aligned MoS₂ Catalysts for Enhanced Hydrogen Evolution. *Nano Res.* 2015;8:566–575. Available from: <https://doi.org/10.1007/s12274-014-0677-7>.
26. Ye G, Gong Y, Lin J, Li B, He Y, Pantelides ST, Zhou W, Vajtai R, Ajayan PM. Defects Engineered Monolayer MoS₂ for Improved Hydrogen Evolution Reaction. *Nano Lett.* 2016;16:1097–1103. PMID: 26761422. Available from: <https://doi.org/10.1021/acs.nanolett.5b04331>.
27. Shokhen V, Zitoun D. Platinum-Group Metal Grown on Vertically Aligned MoS₂ as Electrocatalysts for Hydrogen Evolution Reaction. *Electrochimica Acta.* 2017;257:49–55. Available from: <https://doi.org/10.1016/j.electacta.2017.10.014>.